

Estimation of Biophysical Characteristics for *Chlamydomonas reinhardtii* Pigment Mutants with an M-PEA-2 Fluorometer

D. N. Matorin^a, F. F. Protopopov^{a, b}, A. K. Sadvakasova^c, A. A. Alekseev^b,
L. B. Bratkovskaja^a, and B. K. Zayadan^c

^aDepartment of Biology, Moscow State University, Moscow, 119991 Russia

^bInstitute of Physics and Technology, Ammosov North-Eastern Federal University,
ul. Kulakovskogo 48, Yakutsk, 677000 Russia;

^cAl-Farabi Kazakh National University, pr. Al-Farabi 71, Almaty, 050040, Republic of Kazakhstan

*e-mail: matorin@biophys.msu.ru

**e-mail: protopopov_fedor@mail.ru

***e-mail: sadvakasova1979@mail.ru

Received February 1, 2016

Abstract—Light green pigment mutants with a reduced chlorophyll *b* content were constructed in the microalga *Chlamydomonas reinhardtii* Dangeard. A simultaneous recording of the induction curves for prompt and delayed fluorescence and the redox state of P700 in the microsecond range with a M-PEA-2 fluorometer revealed decreases in the quantum yield of electron transport in PS2 (ϕ_{D_0}) and the performance index (PI_{ABS}) and increases in the quantum efficiency of energy dissipation (ϕ_{D_0}) and ΔpH -dependent non-photochemical quenching (q_E and NPQ). The light-dependence curves of the fluorescence parameters confirmed a decrease in the coefficient of maximum utilization of light energy (α) for the mutants. However, the mutants showed an adequate rate of electron transport at a medium light intensity under steady-state conditions. The mutations did not directly affect the oxidation reactions of the PS1 pigment (P700) and the decrease in delayed fluorescence. Experience in using the mutants to test polluted waters of Kazakhstan confirmed that the mutants are promising for use in biomonitoring for mutagens.

Keywords: prompt and delayed chlorophyll *a* fluorescence, biomonitoring, *Chlamydomonas reinhardtii*, JIP test, M-PEA-2

DOI: 10.1134/S0006350916040151

INTRODUCTION

Microalgae are among the main organisms for biomonitoring to evaluate the toxicity of water environments [1]. Fluorescence methods have been recently employed in biotesting to monitor the state of algae [2, 3]. Fluorescence methods can be used to examine natural algal populations in biomonitoring [1]. A fluorescence method to measure the abundance and to detect changes in phytoplankton in natural waters has been developed at the Department of Biophysics at Moscow State University and has been approved for use in state ecological monitoring within the section “Quantitative Chemical Analysis of Waters” [4].

Fluorescence methods to estimate the activity of the photosynthetic system can provide detailed information on early alterations in cell metabolism mostly at the membrane level [5, 6]. The methods can yield

real-time data on the state of microalgae. Chlorophyll contained in algal membranes serves as a natural indicator of cell photosynthetic activity owing to its fluorescence.

The unicellular green alga *Chlamydomonas reinhardtii* Dangeard is used as a model organism in genetics and is convenient for detecting the effects of various pollutants, including mutagens, on algal populations [1]. With *Chl. reinhardtii*, polluted waters can be tested not only for toxicity, but also for mutagenic activity.

In this work, mutant *Chl. reinhardtii* strains were obtained by induced mutagenesis and tested for photosystem 1 (PS1) and 2 (PS2) activities via spectral methods and a M-PEA-2 fluorometer (Hansa-Tech, United Kingdom). Pigment mutants were found to be promising for use in biotesting water ecosystems for mutagens by detecting green revertants.

Abbreviations: PS1, photosystem 1; PS2, photosystem 2; DF, delayed fluorescence; ETR, relative noncyclic electron transport rate.

MATERIALS AND METHODS

To obtain mutants, *Chl. reinhardtii* cells were exposed to UV light with a wavelength of 254 nm (40 erg/mm^2). After exposure, the suspension was transferred into Petri dishes with the L2-min medium. The cultures were incubated in the light ($120 \mu\text{E/m}^2 \text{ s}$) and examined 10–14 days after seeding. A total of 12 mutant subclones were chosen for further experiments by colony shape and size and subjected to up to ten consecutive cycles of further selection. Three out of the 12 subclones were chosen in multiple selection rounds as they preserved the features acquired as a result of induced mutagenesis. To test the subclones, genetic experiments were carried out using macrocolony and microcolony methods [7].

The fluorescence parameters of algal cells were measured with a Water-PAM pulse fluorometer (Walz, Effelrich, Germany). Dark-adapted samples were used to measure constant (F_O) and maximum (F_M) fluorescence and the maximum variable fluorescence yield $F_V/F_M = F_M - F_O/F_M$, which is a measure of the potential quantum efficiency of PS2. The light dependences of various fluorescence parameters were measured in the light, consecutively increasing the light intensity from 0 to $800 \mu\text{E/m}^2 \text{ s}$ [8]. The duration of light exposure was 50 s. At the end of each light exposure at a certain light intensity, a saturating light flash (0.8 s , $3000 \mu\text{E/m}^2 \text{ s}$) was used to record F'_M and the fluorescence yield in the light $F(t)$. The parameters were used to calculate the nonphotochemical fluorescence quenching $NPQ = (F_M - F'_M)/F'_M$, the quantum yield of chemical transformation of absorbed light energy in PS2 as the ratio $Y = (F'_M - F_t)/F'_M$, and the relative rate of noncyclic electron transport (ETR) at a given light intensity. The electron-transport rate was calculated as $ETR = YE_i/0.5$, where E_i is the light intensity. The resulting ETR light dependence curves were used to estimate the following parameters of photosynthesis: the coefficient of maximum utilization of light energy (slope, α) and the maximum relative electron-transport rate in the electron-transport chain (ETR_{max}). The coefficient α was obtained as the coefficient of linear regression based on points falling in the light-limited region of the P/E curve. The designations and definitions of the photosynthesis parameters follow the conventional nomenclature [8].

Induction curves for prompt and delayed fluorescence and the redox state of P700 were recorded simultaneously using a Multifunction Plant Efficiency Analyzer (M-PEA-2, Hansatech Instruments, United Kingdom) [5, 6, 9]. Prompt and delayed fluorescence measurements were performed with alternating periods of illumination with actinic red light ($1300 \mu\text{E/m}^2 \text{ s}$, a spectral maximum at 625 nm) and short dark periods sufficient for detecting delayed fluorescence

(DF). The fluorescence-induction kinetics was measured with a time resolution of 0.01 ms. Changes in absorption at 820 nm are thought to reflect the redox state of P700, a PS1 reaction center [6, 10]. The intensity of modulating light with a peak at $820 \times 25 \text{ nm}$ was chosen to be $1000 \mu\text{E/m}^2 \text{ s}$. Modulated reflection (MR) data were normalized to MR at $t = 0.7 \text{ ms}$ (MR_O) [6]. The total duration of one measurement was 60 s. The DF dynamics reflected changes in fluorescence intensity on a scale of 0.1–0.9 ms in intervals between actinic light pulses. The characteristics and measurement protocol have been described for the M-PEA-2 instrument in [9–11]. Prior to measurements, algal samples were concentrated on a membrane filter and exposed in the dark for 10 min while keeping them wet.

The so-called JIP test was used to quantitatively analyze the characteristics of primary photosynthetic processes on the basis of the fluorescence induction curves [6, 9, 12]. The following parameters of a fluorescence induction kinetic curve are used in the JIP test: intensities at 20 ms (F_O), 2 ms (F_J), 30 ms (F_t), and 6 s (F_{6s}); F_P (F_M , maximum fluorescence intensity); and *Area* (the area above the OJIP kinetic curve and below the F_M level).

These measurable values were used to calculate the following parameters:

$F_V = F_M - F_O$ is the maximum variable fluorescence;

F_V/F_M is the maximum quantum yield of the primary photochemical reaction in open reaction centers of PS2, $F_V/F_M = \phi P_O = TR_O/ABS$;

ϕE_O is the quantum yield of electron transport (at $t = 0$): $\phi E_O = ET_O/ABS = (TR_O/ABS)(ET_O/TR_O) = [1 - (F_O/F_M)](1 - V_J)$, where $V_J = (F_J - F_O)/F_V$;

ϕD_O is the quantum yield of energy dissipation: $\phi D_O = 1 - \phi P_O = (F_O/F_M)$;

ABS/RC is the energy flux absorbed per one active reaction center and characterizes the relative antenna size: $ABS/RC = (TR_O/RC)/(TR_O/ABS) = M_O/V_J(1/\phi P_O) = (M_O/V_J)/[(F_M - F_O)/F_M]$;

PI_{ABS} is the performance index, that is, PS2 functional activity related to the energy absorbed: $PI_{\text{ABS}} = [1 - (F_O/F_M)]/(M_O/V_J)[(F_M - F_O)/F_O][(1 - V_J)/V_J]$;

q_E is the potential for pH-induced nonphotochemical fluorescence quenching: $q_E = (F_M - F_{6s})/F_V$;

S_M is the normalized area over the OJIP curve and reflects the total pool of electron transporters from time $t = 0$ to time t_{F_M} (the time to maximum fluorescence): $S_M = \text{Area}/F_V$.

Light absorption spectra were recorded using a HITACHI double-beam spectrophotometer (Hitachi, Japan). Fluorescence excitation spectra were recorded using a Fluorolog-3 spectrofluorometer (Horiba Jobin Yvon S.A.S., France) with time-correlated single pho-

ton counting (TCSPC). Fluorescence was excited using a pulse light-emission diode (LED) with a range of 390–700 nm and measured at 685 nm.

All measurements were repeated at least five times; mean values are reported.

RESULTS

The clones obtained in autotrophic conditions were light green pigment mutants, which were designated CC-124y-1, CC-124y-2, and CC-124p-2. The strains were similar in cultural and morphological characteristics, were 2.0–3.5 mm in size, and produced light green colonies on a solid medium. The cells had two flagella of the same length at the anterior end. Chlorophyll was totally contained in a chromatophore. Cultures grew well in liquid and agar L-min media in photoautotrophic conditions at an air temperature of 22–30°C.

Figure 1 shows the absorption spectra of the wild-type *Chl. reinhardtii* strain and the CC-124y-2 and CC-124p-2 mutants. The CC-124y-2 strain has been described previously [13]. The spectra were normalized to the maximum absorption by chlorophyll *a* at 675 nm. A substantial decrease in absorption in the region of 650 nm was observed for the CC-124y-2 and CC-124p-2 mutants compared with the wild-type strain, indicating that their chlorophyll *b* contents were several times lower than the chlorophyll *a* content. This finding is supported by fluorescence excitation spectra (Fig. 1b).

A decrease in absorption in the carotenoid region (450–500 nm) was additionally observed in the absorption spectra of the CC-124y-2 and CC-124p-2 mutants (Fig. 1a). Similar changes were even greater in the fluorescence excitation spectra (Fig. 1b). The finding indicates that the carotenoid content was substantially reduced in the CC-124y-2 and CC-124p-2 mutants.

As is well known, carotenoids do not fluoresce in algae, but efficiently transfer their excitation energy to chlorophyll *a*, which is a major source of fluorescence. A greater decrease at 450–500 nm in the fluorescence excitation spectra compared with the absorption spectra points to a poorer association of carotenoids with fluorescing chlorophyll *a* in the CC-124y-2 and CC-124p-2 mutants.

The ratio between the fluorescence intensities measured on exposure to photosynthesis-saturating light (F_M) and in conditions that do not change the state of the photosynthesizing system (a low light intensity, F_0) makes it possible to characterize the maximum efficiency of PS2 processes as $(F_M - F_0)/F_M = F_V/F_M$ [8]. The F_V/F_M ratio is a dimensionless characteristic of photosynthesis that is similar to the coefficient of performance. The maximum quantum yield of primary photochemistry $F_V/F_M (\phi_{P_0})$ was

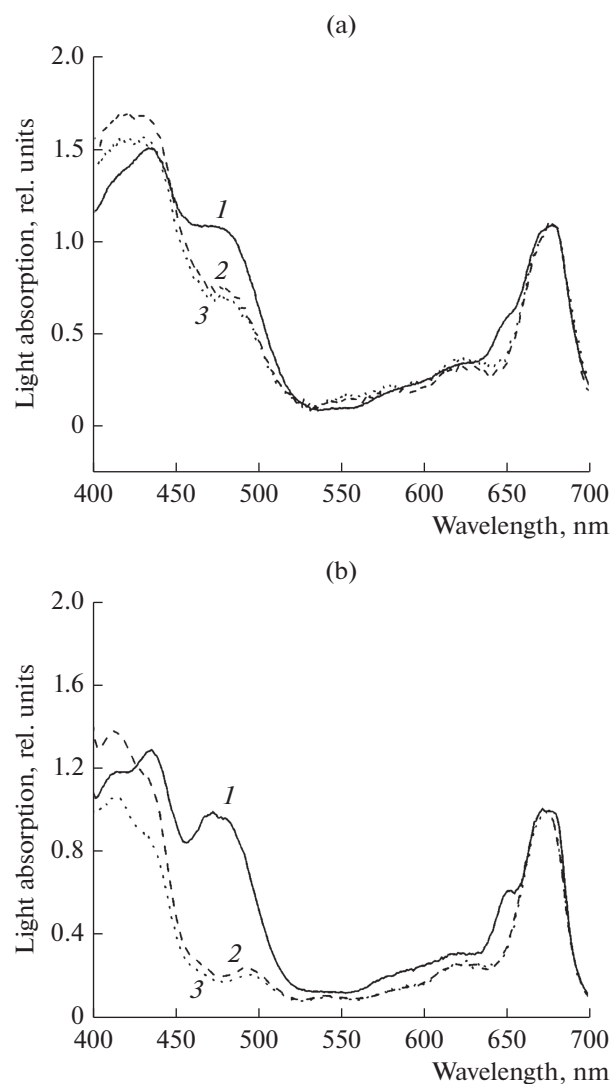


Fig. 1. (a) Absorption and (b) fluorescence excitation spectra of (1) the wild-type *Chl. reinhardtii* strain (CC-124) and the (2) CC-124p-2 and (3) CC-124y-2 mutants. The spectra were normalized to the red chlorophyll *a* maximum at 675 nm.

high (0.728) in the wild-type *Chl. reinhardtii* strain and somewhat lower in the CC-124y-2 and CC-124p-2 mutants.

Fluorescence induction curves obtained with a high time resolution (10 ms and higher) on excitation with intense light have recently come into use to evaluate the function of the photosynthetic system in higher plants and algal cultures [5, 6]. Recording high-resolution fluorescence induction curves takes only a few seconds and is done using instruments similar to PAM or PEA. The M-PEA-2 instrument makes it possible not only to record chlorophyll fluorescence, but also to simultaneously measure the modulated reflection at 820 nm, which characterizes the redox state of the P700 pigment of the PS1 reaction center.

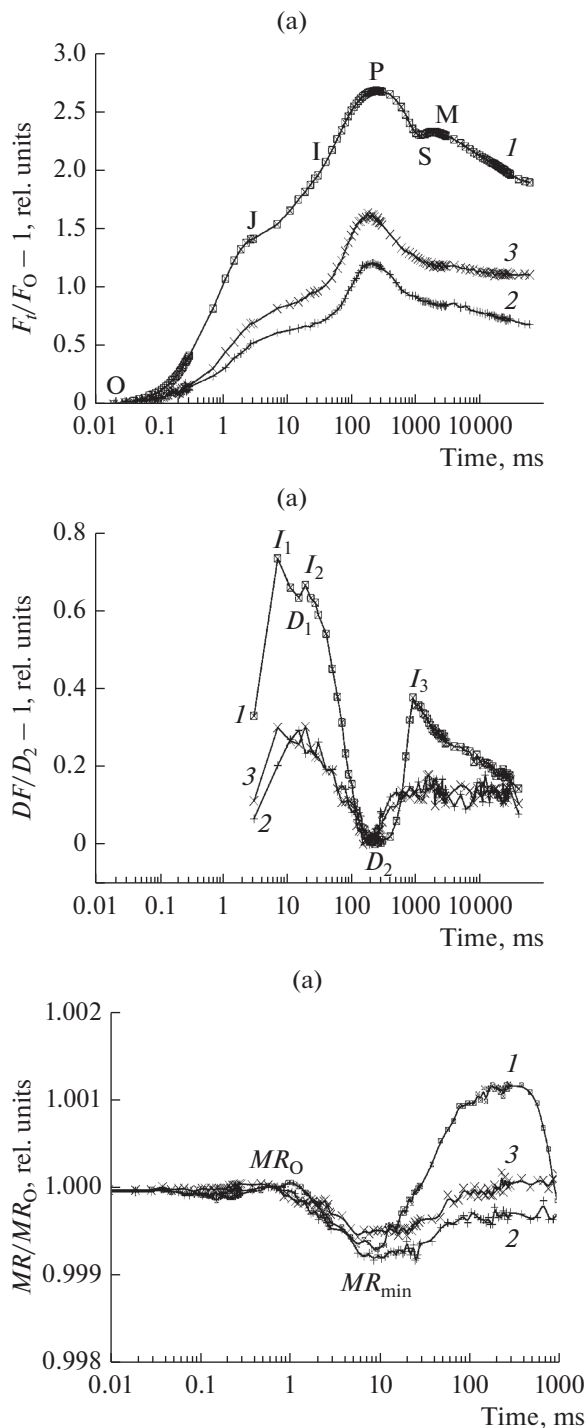


Fig. 2. Induction curves of (a) prompt fluorescence and (b) DF and (c) changes in reflection at 820 nm as measured for (1) the *Chl. reinhardtii* wild-type strain and the (2) CC-124p-2 and (3) CC-124y-2 mutants. Prompt fluorescence and DF curves were normalized to F_0 and D_2 , respectively. The actinic red light intensity was $1300 \mu\text{E}/\text{m}^2 \text{ s}$. The three signals were simultaneously measured with a M-PEA-2 instrument.

In other words, the instrument allows the monitoring of particular reactions in PS2 and PS1 and a simultaneous recording of induction changes in DF [5, 6, 9].

To characterize the changes in the photosynthetic system of the mutants in detail, we measured the induction curves of prompt fluorescence and DF and the redox state of P700. The prompt fluorescence kinetic induction curves normalized to F_0 are shown in Fig. 2a. The kinetic curve obtained for wild-type cells agreed with curves reported in the literature [9, 12]. Several phases, which are known as the O–J–I–P transitions, are seen in the induction curve obtained for prompt fluorescence on exposure to light [9]. The initial level O corresponds to the chlorophyll fluorescence intensity when PS2 reaction centers are open (F_0) and all Q_A acceptors are oxidized. Phase O–J is due to light-induced reduction of the Q_A acceptor, and the following phases mostly reflect a further accumulation of reduced Q_A^- , which accumulates because its re-oxidation decreases as Q_B acceptors and the quinone pool are reduced.

The fluorescence induction curves for the CC-124y-2 and CC-124p-2 mutants differed from the curve of the wild-type strain. Variable fluorescence F_V ($F_V = F_M - F_0$) was lower in the mutants, mostly because the maximum fluorescence F_M was decreased. To quantitatively analyze the characteristics of primary photosynthetic processes on the basis of the O–J–I–P kinetic curve parameters, we used the JIP test with the parameters described in the Materials and Methods.

The ABS/RC parameter in the CC-124y-2 and CC-124p-2 mutants was higher than in wild-type cells because the mutants have a lower portion of active reaction centers relative to the absorbed light. The quantum yield of the electron transport in PS2 (ϕ_{E_0}) was decreased in the mutant strains. The parameter S_M , which reflects the relative size of the electron acceptor pool in PS2, in the mutants was higher than in the wild-type strain.

The index PI_{ABS} reflects the PS2 functional activity related to the energy absorbed. The index for wild-type cells was higher than in the mutant strains. Lower PI_{ABS} values indicate that PS2 functional activity in the mutants was decreased, mostly because the portion of active reaction centers was lower and the quenching of excited states in the antenna to produce heat (ϕ_{D_0}) was higher. A decrease in the efficiency of excitation energy transfer from the light-absorbing complex to the reaction center should be accompanied by an increase in dissipation of unused light energy. In fact, the quantum efficiency of energy dissipation (ϕ_{D_0}) was high in the mutants. Its high values correlated with an increase in ΔpH -dependent nonphotochemical quenching q_E , which is obtained from the

decrease in fluorescence after its maximum ($q_E = (F_M - F_{6s})/F_V$).

Simultaneous measurements of the modulated reflection at 820 nm showed that photoinduced oxidation of P700 took place in dark-adapted cells. A maximum P700⁺ accumulation was observed at $t \approx 30$ ms (MR_{\min}), after which P700 was reduced (Fig. 2b). The fluorescent signal reflecting Q_A reduction and the P700 reduction processes were leveled almost synchronously. The parallel accumulation of the reduced forms of P700 and Q_A reflects reduction of transporters throughout the electron transport chain region between the photosystems; this reduction is due to lack of electron efflux from the acceptor part of PS1 in conditions where ferredoxin–NADP reductase is inactivated by cell incubation in the dark. Another wave of P700 oxidation was observed upon a prolonged exposure to light (~ 1 – 10 s) and could be explained by electron efflux from PS1, which arises with activation of ferredoxin–NADP reductase and enzymes of the Calvin cycle.

As is seen from Fig. 2c, P700 preserved the capability of oxidation on exposure to light in the CC-124y-2 and CC-124p-2 mutants. However, the P700 reduction rate of PS2 was decreased in the mutants. The finding agrees with the results of analyzing the induction curves of prompt fluorescence.

Millisecond DF results from the secondary charge recombination reaction and its intensity depends on the electrochemical proton gradient across the thylakoid membrane because the gradient energy decreases the activation energy of the reverse charge recombination reaction [5, 6]. Hence, DF recording is a method to monitor the proton gradient across the cell membrane. A maximum of the DF curve in the millisecond range (I_1) coincides with phase I–J of increasing fluorescence on the induction curve of prompt fluorescence (Fig. 2a). Peaks I_1 and I_2 are due to an accumulation of certain radiative redox states responsible for reverse charge recombination and emission of DF quanta (i.e., emitting states) and to an increase in DF, which arises because an electrical potential ($\Delta\psi$) is generated on the membrane. The third peak I_3 , which is in the second range, is associated with the photoinduced generation of a transmembrane proton gradient (ΔpH), which also decreases the activation energy of radiative transitions (DF emission) in the reaction center of PS2. These regularities have been considered in many studies [5, 6].

In the CC-124y-2 and CC-124p-2 mutants, a lower DF intensity on the induction curve was observed at 10–50 ms (DF peaks I_1 and I_2) and 1 s (DF peak I_3). The decreases are probably related to a substantial decrease in noncyclic transport and, consequently, lower photosynthetic membrane energization.

Thus, a simultaneous recording of the prompt fluorescence and DF induction curves and the changes in

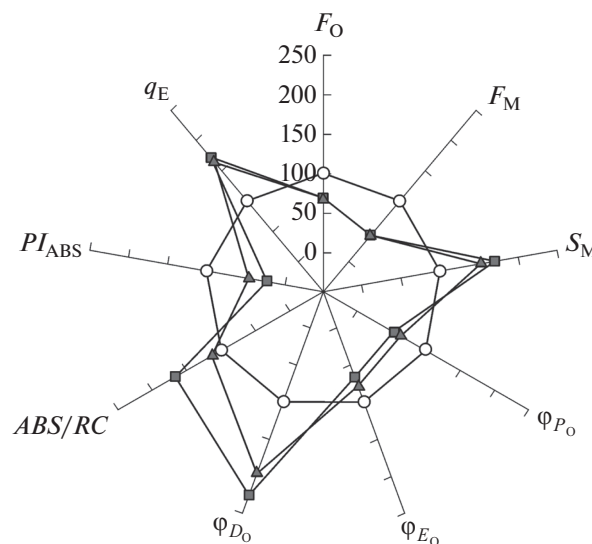


Fig. 3. A diagram of the JIP-test parameters based on the induction curve of prompt fluorescence. The parameters were obtained for the wild-type CC-124 *Chl. reinhardtii* strain (circles) and the CC-124p-2 (squares) and CC-124y-2 (triangles) mutants and normalized to the wild-type cell parameters; the values are shown in percent.

redox states of P700 with M-PEA-2 made it possible to monitor particular reactions with an accumulation of reduced inter-photosystem transporters, switching on of PS1, and the kinetics of the electrochemical proton gradient across the thylakoid membrane in the mutants.

Measuring the light-dependence curves for fluorescence parameters finds increasing application in ecological and physiological studies of photosynthesis [5, 8]. The quantum yield Y of the photochemical conversion of absorbed light energy in PS2 in the light is defined as $Y = (F'_M - F)/F'_M$. With Y known, the relative noncyclic electron transport rate (ETR) can be obtained as a multiple of the light intensity and Y (see Materials and Methods). Light-dependence curves of the relative ETR of the algal strains are shown in Fig. 4a. The relative ETRs of the mutants were lower than the control at light intensities of up to $200 \mu E/m^2 s$. However, the ETRs of the mutants were somewhat higher than the ETR of the wild-type strain in the actinic light intensity range 400 – $800 \mu E/m^2 s$. The latter finding indicates that a sufficient electron transport level was preserved in the mutants at a moderate light intensity under steady-state conditions. A light dependence curve can be used to estimate the coefficient of maximum utilization of light energy as the slope α of the linear region of the curve. The coefficient α of maximum utilization of light energy was decreased in the mutants; the finding agreed with the changes inferred for the electron transport system from the fluorescence-induction curves.

Genetic toxicity testing of wastewaters from Almaty car washes and the Pavlodar Oil Refinery using the wild-type and CC-124y-2 mutant *Chl. reinhardtii* strains

Test water	Frequency	Control (number of colonies)	Experiment (sample no.), number of colonies per 10 ⁵ colonies	
			1	2
Wastewaters from Almaty car washes	Pigment mutants in the wild-type strain	0	0	0
	Revertants in the mutant strain	0	0	0
Wastewaters from the Pavlodar Oil Refinery	Pigment mutants in the wild-type strain	0	9 ± 1	26 ± 1
	Revertants in the mutant strain	0	28 ± 1	63 ± 2

A decrease in the quantum yield Y of PS2 photochemistry in algae at a higher light intensity is associated with an increase in the dissipation of excessive light energy as heat, as the energy cannot be utilized in light reactions. The process is reflected in nonphotochemical quenching of fluorescence on exposure to actinic light and is calculated as $NPQ = (F_M/F'_M) - 1$ [8]. The nonphotochemical quenching NPQ decreased in the mutants at lower actinic light intensities (below 200 $\mu\text{E}/\text{m}^2 \text{ s}$) and increased in the range of 400–800 $\mu\text{E}/\text{m}^2 \text{ s}$. It is important to note that this correlated with an increase in the ΔpH -dependent nonphotochemical quenching q_E (Fig. 2).

An example of using the mutants to test waters for genetic toxicity. Our color mutants can be employed in

biomonitoring of natural and waste waters. As an example, the strains were used to assess the genetic toxicity of wastewaters from an Almaty car wash and the Pavlodar Oil Refinery (table). Cells of the wild-type and CC-124y-2 mutant *Chl. reinhardtii* strains were incubated in test water samples and then examined for the frequency of direct mutants and revertants, respectively. A revertant is a mutant that expresses partly or completely restored traits of the original wild-type strain (e.g., a green cell color) as a result of a suppressor or compensatory reverse mutation.

Estimations were performed by a macrocolony method, which is common in microbiology. To estimate the cell viability and the mutation frequency, a certain number of cells were seeded in Petri dishes

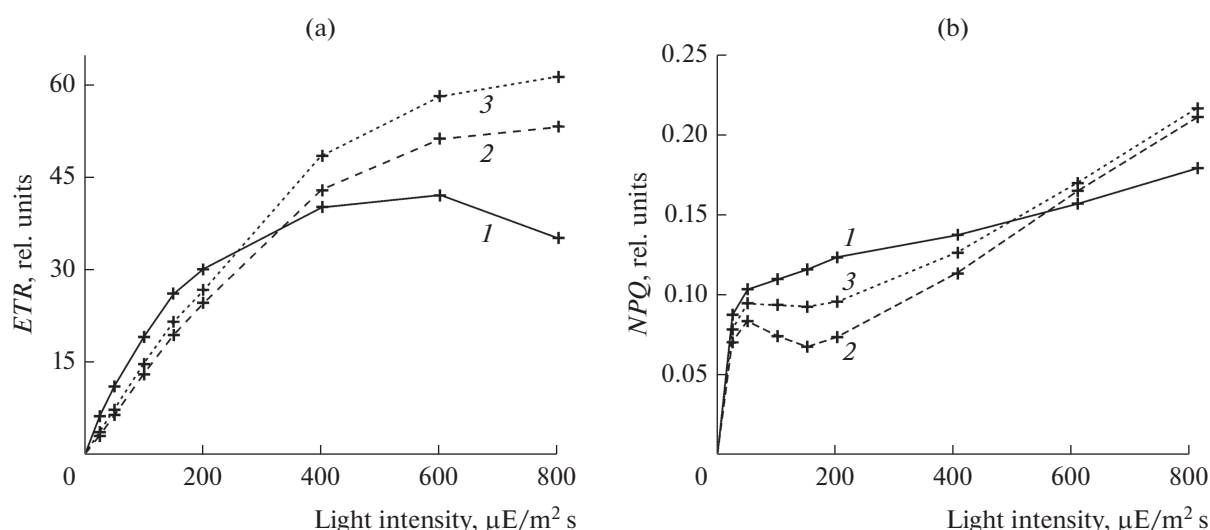


Fig. 4. Fluorescence parameters as functions of actinic light intensity in (1) the wild-type CC-124 *Chl. reinhardtii* strain and the (2) CC-124p-2 and (3) CC-124y-2 mutants. (a) Relative electron transport rate (ETR) and (b) nonphotochemical quenching (NPQ).

with an agar medium at 200–500 cells per dish. The dishes were incubated in a climate chamber for 7–10 days. The surviving colonies were then counted (CFU/mL) and the frequency of mutants was estimated by colony color [14]. Pigment mutants of the wild-type strain and revertants of the pigment mutant were not observed in cultures exposed to wastewaters of Almaty car washes (table). This result indicates that the test samples had no mutagenic activity toward *Chl. reinhardtii*.

When wastewaters from the Pavlodar Oil Refinery were tested, direct mutants and revertants were detected by colony color, suggesting mutagenic activity for test wastewaters. Thus, the study showed that the light green mutants with a low chlorophyll *b* content are promising to employ in testing the ecological status of natural and waste waters.

DISCUSSION

The system with microalgae to assess water quality is promising and can be further improved by developing new mutant strains or extending the range of mutants to include, for example, strains that lack chlorophyll *b*, have no envelope, are sensitive to light, or have defects in the cell-repair system [14–16].

Such promising mutants with a lower chlorophyll *b* content were obtained and characterized in this work. Studies with the M-PEA-2 instrument revealed specific changes in PS2 reactions and P700 oxidation in the mutant strains. A simultaneous recording of the induction curves for prompt and delayed fluorescence and the redox state of P700 in the microsecond range with M-PEA-2 showed decreases in the quantum yield of electron transport in PS2 (ϕ_{E_0}) and performance index (PI_{ABS}) and increases in the quantum efficiency of energy dissipation (ϕ_{D_0}) and ΔpH -dependent nonphotochemical quenching (q_E and NPQ).

The light-dependence curves of the fluorescence parameters confirmed the changes in the electron transport chain for the mutants. The coefficient of maximum utilization of light energy (α) was decreased in the mutants. However, the mutants showed an adequate rate of electron transport at a medium light intensity under steady-state conditions. The mutations did not directly affect the oxidation reactions of the PS1 pigment (P700) and the decrease in delayed fluorescence.

Our results indicate that changes in the induction curves of prompt and delayed fluorescence are among the primary parameters that can be rapidly recorded for algal cells after mutagenesis. These parameters can be efficiently used to diagnose the status of test organisms. The results provide a better understanding of the mechanisms that regulate the primary processes in PS1 and PS2 and demonstrate that various fluores-

cence parameters can be employed in biotesting water in natural and artificial water bodies. Our pigment mutants that lack chlorophyll *b* are promising for use in testing the ecological status of polluted water ecosystems. The pigment composition as a genetic criterion provides a valuable advantage when the mutants are employed in genetic environmental monitoring to test environments for mutagenicity.

Experience in using the mutants to test polluted waters of Kazakhstan confirmed that the mutants are promising for use in biomonitoring for mutagens.

ACKNOWLEDGMENTS

We are grateful to E.P. Lukashov (Department of Biophysics, Moscow State University) for help in spectral studies.

This work was supported by the Kazakh Foundation for Basic Research (project no. GF2015, state registration no. 015RK00290), the Ministry of Education and Science of Kazakhstan (project no. 1582/GF4 to B.K. Zayadan), and the Russian Foundation for Basic Research (project no. 14-0400143).

REFERENCES

1. B. K. Zayadan and D. N. Matorin, *Aquatic Ecosystem Monitoring Based on Microalgae* (Alteks, Moscow, 2015) [in Russian].
2. N. S. Zhmur and T. L. Orlova, *Procedure of Determining the Toxicity of Waters, Water Extracts of Soils, Sewage Sludge, and Wastewater from Changes in the Level of Chlorophyll Fluorescence and the Numbers of Algal cells, FR. 1.39.2007.03223* (Akvaros, Moscow, 2007) [in Russian].
3. Yu. S. Grigor'ev and E. S. Sravinskiene, *Procedure of Measuring the Relative Index of Delayed Fluorescence of *Chlorella vulgaris* Beijer Culture for Determining the Toxicity of Drinking Waters, Natural Fresh Waters, Wastewaters, Water Extracts from Soils, Sewage Sludge, and Industrial and Consumer Wastes* (PND F T 14.1:2.4.16-09; PND F T 16.1:2.3:3.14-09, 2014) [in Russian].
4. D. N. Matorin, V. A. Osipov, and A. B. Rubin, *Procedure of Measuring the Abundance of Phytoplankton and Changes in Its State in Natural Waters by a Fluorescent Method: Theoretical and Practical Aspects. A Manual* (Alteks, Moscow, 2012) [in Russian].
5. D. N. Matorin and A. B. Rubin, *Fluorescence of Chlorophyll from Higher Plants and Algae* (IKI-RKhD, Izhevsk, 2012) [in Russian].
6. V. N. Goltsev, M. Kh. Kaladzhi, M. A. Kuzmanova, and S. I. Allakhverdiev, *Variable and Delayed Fluorescence of Chlorophyll *a*: Theoretical Aspects and Applications in Studies on Plants* (IKI-RKhD, Izhevsk, 2014) [in Russian].
7. B. K. Zayadan, A. K. Sadvakasova, M. M. Saleh, and M. M. Gaballah, *Int. J. Curr. Microbiol. Appl. Sci.* **2** (12), 64 (2013).
8. U. Schreiber, in *Chlorophyll Fluorescence: A Signature of Photosynthesis*, Ed. by G. Papageorgiou and Govindjee

- (Springer, Dordrecht, Netherlands, 2004), pp. 279–319.
9. R. J. Strasser, M. Tsimilli-Michael, S. Qiang, and V. Goltsev, *Biochim. Biophys. Acta* **1797**, 1313 (2010).
 10. A. A. Bulychiev, V. A. Osipov, D. N. Matorin, and W. J. Vredenberg, *J. Bioenerg. Biomembr.* **45**, 37 (2013).
 11. V. V. Lenbaum, A. A. Bulychiev, and D. N. Matorin, *Russ. J. Plant Physiol.* **62** (2), 210 (2015).
 12. D. Lazar and G. Schansker, in *Photosynthesis in Silico* (Springer, Netherlands, 2009), pp. 85–123.
 13. A. K. Sadvakasova, N. R. Akpukhanova, B. K. Zayadan, et al., *Russ. J. Plant Physiol.* **63** (4) (2016).
 14. K. V. Kvitko, I. A. Zakharov, and V. I. Khropova, *Genetika* No. 2, 148 (1966).
 15. G. Mijlt, B. K. Zayadan, E. Rahman, et al., *Acta Genetica Sinica* **30** (7), 646 (2013).
 16. A. V. Stolbova, Yu. V. Nakonechnyi, O. N. Mirnaya, and V. V. Tugarinov, *Izv. St.-Peterb. Gos. Univ.* **3** (4), 111 (1995).

Translated by T. Tkacheva

SPELL: 1. OK